

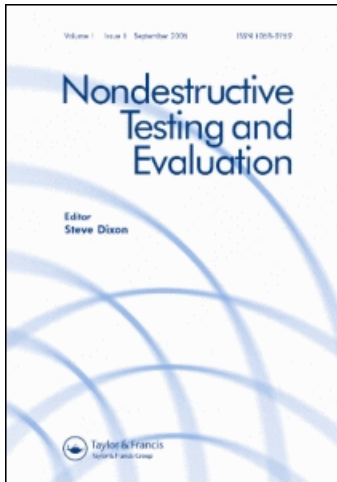
This article was downloaded by: [Ruben, Specogna]

On: 22 December 2008

Access details: Access Details: [subscription number 907124640]

Publisher Taylor & Francis

Informa Ltd Registered in England and Wales Registered Number: 1072954 Registered office: Mortimer House, 37-41 Mortimer Street, London W1T 3JH, UK



## Nondestructive Testing and Evaluation

Publication details, including instructions for authors and subscription information:

<http://www.informaworld.com/smpp/title-content=t713645777>

### Advanced geometric formulations for the design of a long defects detection system

Ruben Specogna <sup>a</sup>; Francesco Trevisan <sup>a</sup>

<sup>a</sup> University of Udine, Udine, Italy

First Published: March 2009

**To cite this Article** Specogna, Ruben and Trevisan, Francesco (2009) 'Advanced geometric formulations for the design of a long defects detection system', *Nondestructive Testing and Evaluation*, 24:1, 195 — 207

**To link to this Article:** DOI: 10.1080/10589750802213494

**URL:** <http://dx.doi.org/10.1080/10589750802213494>

PLEASE SCROLL DOWN FOR ARTICLE

Full terms and conditions of use: <http://www.informaworld.com/terms-and-conditions-of-access.pdf>

This article may be used for research, teaching and private study purposes. Any substantial or systematic reproduction, re-distribution, re-selling, loan or sub-licensing, systematic supply or distribution in any form to anyone is expressly forbidden.

The publisher does not give any warranty express or implied or make any representation that the contents will be complete or accurate or up to date. The accuracy of any instructions, formulae and drug doses should be independently verified with primary sources. The publisher shall not be liable for any loss, actions, claims, proceedings, demand or costs or damages whatsoever or howsoever caused arising directly or indirectly in connection with or arising out of the use of this material.

## Advanced geometric formulations for the design of a long defects detection system

Ruben Specogna\* and Francesco Trevisan

*University of Udine, via delle Scienze 208, 33100 Udine, Italy*

*(Received 29 February 2008; final version received 19 May 2008)*

The aim of the paper is to highlight some of the innovative methodologies, techniques and systems for nondestructive electromagnetic testing, which have been developed in the framework of the applications of methods of a diagnostics electromagnetic project partially funded by the Italian Ministry of University and Research.

In particular, we will present the feasibility design of a suitable exciting-receiving coils configuration able to detect long defects by means of eddy-currents. To solve the forward eddy-currents problem, advanced analysis tools have been developed and validated.

**Keywords:** nondestructive testing; eddy-currents; discrete approaches

### 1. Introduction

The strong international industrial competition forced industrial companies to optimise the manufacturing processes, in order to reduce the overall manufacturing time. One of the conditions to be satisfied for this goal is the capability to detect very quickly the product non-conformities with respect to the assumed standards.

For these reasons, there is a remarkable interest in the techniques for the detection of the surface defects that can be present during the hot mill rolling process of the steel bars with circular cross-section (with a diameter from 8 to 80 mm, a speed from 5 to 100 m/s in the longitudinal direction and a temperature from 800 to 1200°C).

The capability to detect these defects permits a fast and straightforward quality assessment of the product and provides the possibility to reduce those defects due to a wrong set-up of the manufacturing process parameters. The defects considered have a depth ranging from 0.1 to 2 mm and, even though they have quite different shapes and sizes, they generally correspond to an interruption of the material continuity (also from the electrical point of view) and lay along an almost axial direction. Two main categories of surface defects can be considered depending on their axial length  $L$ : the 'short' defects, with  $L$  ranging from 1 to 20 mm and the 'long' defects with  $L$  from a metre to tens of metres. In any case, the defect width is much smaller than the two other dimensions. Short defects can be easily detected using a differential method in which the signal, after the noise reduction, is compared to a similar signal taken few centimetres away along the axial direction. On the contrary, so far, no practical solution has been found as regards to the detection of long defects, for which a differential approach is not suitable.

The motivation of this paper is to develop the feasibility design of an exciting-receiving coil configuration able to detect the long defects. The numerical simulations have been performed with a discrete geometric approach [1–4] based on the so-called  $A-\chi$  and  $T-\Omega$  formulations<sup>1</sup>

---

\*Corresponding author. Email: ruben.specogna@uniud.it

described in [5,7,10] and modified in order to represent the effect of source currents in an integral way. For numerical comparisons, we used an integral formulation [8].

## 2. Geometric model of the problem

The geometry of the problem consists of a conducting AISI (American Iron and Steel Institute) 310 steel bar, modelled as a conducting cylinder  $D_c$ . The radius of the bar is 17 mm and the conductivity is  $\sigma = 1.236 \times 10^6$  S/m. A longitudinal perfectly insulating defect is assumed, 0.5 mm deep from the surface of the cylinder and 0.2 mm thick. A pair of source coils  $D_s$  (30 mm inner radius, 39 mm outer radius, 1.5 mm height, 7 turns each) are fed by a sinusoidal current of  $I = 200$  mA per turn with a frequency of  $f = 100$  kHz, Figure 1. They are connected in counter series and the distance between the two coils is 30 mm, see Figure 2(a) and (b).

A set of 12 evenly spaced circular-receiving coils (3 mm inner radius, 6.5 mm outer radius, 6 mm height, 400 turns, lift-off 15 mm) with axis directed as the radii of the bar, are considered.

## 3. Solution of the eddy-current problem

### 3.1 Introduction to discrete geometric approach

In order to solve the eddy-current problem we resort to the so-called discrete geometric approach [1–4].

The domain of interest  $D$  of the eddy-current problem has been partitioned into a source region  $D_s$ , consisting of a pair of current-driven coils, and of a passive conductive region  $D_c$ . The complement of  $D_c \cup D_s$  in  $D$  represents the air region  $D_a$ . We assume linearity of media, a permeability  $\mu_0$  in  $D$  and a resistivity  $\rho$  in  $D_c$ .

We introduce in  $D$  a pair of interlocked cell complexes [1,2]. One complex is made of simplexes, i.e., nodes, edges, faces (triangles) and volumes (tetrahedra), while the other is obtained from it, according to the *barycentric* subdivision. Each geometric element of a cell complex is endowed with an orientation [4]. The cell complex whose geometric elements are endowed with *inner* orientation is referred to as the *primal complex* and denoted with  $\mathcal{K}$ . Whereas we denote with  $\tilde{\mathcal{K}}$  the cell complex whose geometric elements are endowed with *outer* orientation, as the same geometric element of a complex can be thought with two

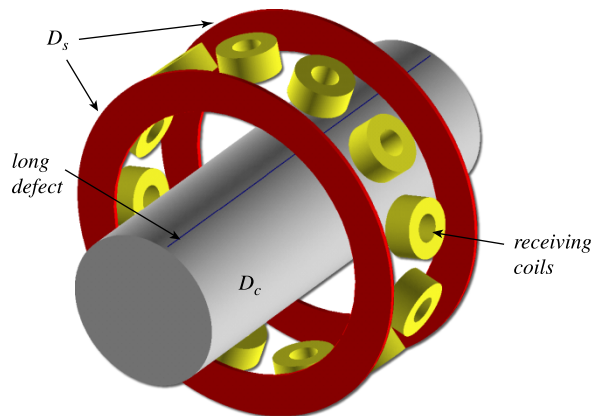


Figure 1. Geometric model of the detection system. It consists of a pair of transmission coils coaxial with the steel bar and 12 evenly spaced circular-receiving coils.

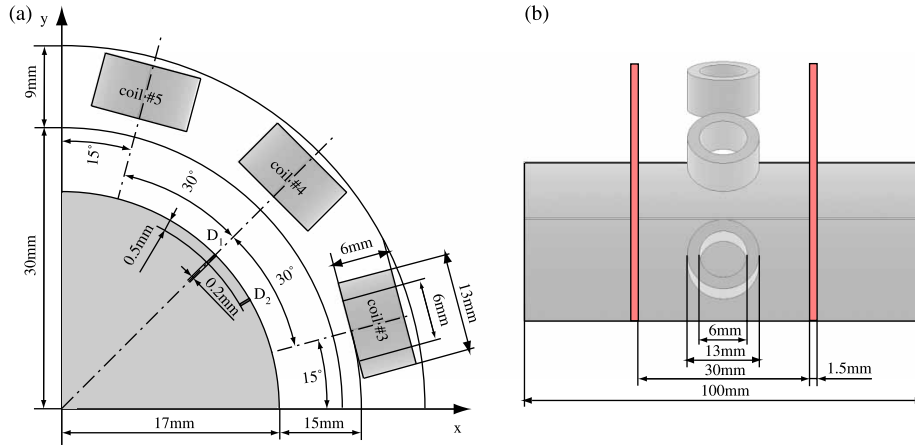


Figure 2. Details of the detection system geometry.

complementary orientations, we may construct two pairs of meshes  $\mathcal{M}' = (\mathcal{K}^s, \tilde{\mathcal{K}})$  and  $\mathcal{M}'' = (\mathcal{K}, \tilde{\mathcal{K}}^s)$ , where the superscript 's' indicates the simplicial complex. The geometric elements of the primal mesh ( $\mathcal{K}^s$  for  $\mathcal{M}'$  or  $\mathcal{K}$  for  $\mathcal{M}''$ ) are denoted with  $n$  for nodes,  $e$  for edges,  $f$  for faces and  $v$  for volumes; whereas the geometric elements of the dual mesh ( $\tilde{\mathcal{K}}$  for  $\mathcal{M}'$  or  $\tilde{\mathcal{K}}^s$  for  $\mathcal{M}''$ ) are denoted with  $\tilde{n}$ ,  $\tilde{e}$ ,  $\tilde{f}$ ,  $\tilde{v}$ , respectively, Figure 3.

The interconnections between the geometric elements of a complex of  $\mathcal{M}'$  or  $\mathcal{M}''$  are described by means of incidence matrices. In particular for the simplicial primal complex  $\mathcal{K}^s$ , we denote with  $\mathbf{G}$  the incidence matrix between the orientations of  $e$  and  $n$ , with  $\mathbf{C}$  the incidence matrix between the orientations of  $f$  and  $e$  and with  $\mathbf{D}$  the incidence matrix between the orientations of  $v$  and  $f$ ; similarly for the simplicial dual complex  $\tilde{\mathcal{K}}^s$  we write  $\tilde{\mathbf{G}}$ ,  $\tilde{\mathbf{C}}$  and  $\tilde{\mathbf{D}}$ , respectively. In particular between the incidence matrices of  $\mathcal{K}^s$  and  $\tilde{\mathcal{K}}^s$  we have that  $\mathbf{G} = -\tilde{\mathbf{G}}^2$ ,  $\mathbf{C} = \tilde{\mathbf{C}}$ ,  $\mathbf{D} = \tilde{\mathbf{D}}$  hold.

Next, we consider the integrals of the field quantities, also referred to as *global variables*, for an eddy-current problem with respect to the oriented geometric elements of a mesh  $\mathcal{M}'$  or  $\mathcal{M}''$ , yielding the degrees of freedom (DoF) arrays (denoted in boldface type); each entry of a DoF array is indexed over the corresponding geometric element. There is a univocal association between a global variable and the corresponding geometric element [4], and we denote them by:

- $\Phi$  the array of magnetic induction fluxes associated with  $f \in D$ ;
- $\mathbf{F}$  the array of magnetomotive forces (m.m.f.s) associated with  $\tilde{e} \in D$ ;
- $\mathbf{I}$  the array of electric currents associated with  $\tilde{f} \in D_c \cup D_s$ . In  $D_s$  we introduce the array  $\mathbf{I}_s$  of impressed currents;
- $\mathbf{U}$  the array of electromotive forces on primal edges  $e \in D_c$ .

With respect to the cell complexes previously defined, we recall the algebraic equations governing the discrete eddy-currents problem in the framework of the discrete geometric approach [5,7,10].

### 3.2 $A-\chi$ formulation

In  $D$  we consider the mesh  $\mathcal{M}'$  and we refer all the incidence matrices to the simplicial complex  $\mathcal{K}^s$ . We denote with:

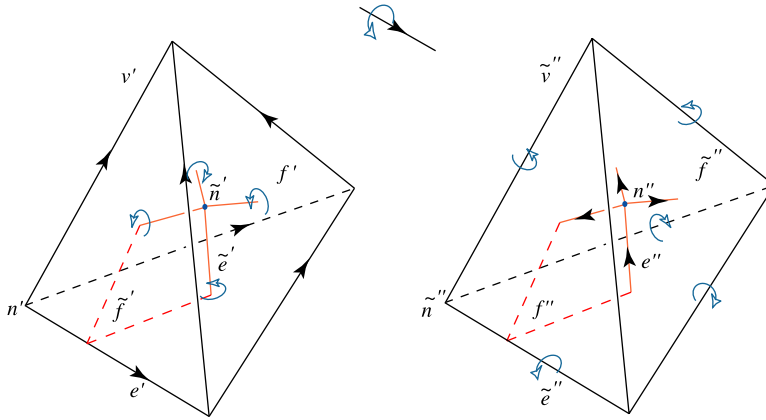


Figure 3. Mesh  $\mathcal{M}'$  is shown on the left side and mesh  $\mathcal{M}''$  on the right.

- $\mathbf{A}$  the array of the circulations  $A$  of the magnetic vector potential along the primal edges  $e \in D$ ;
- $\chi$  the array of electric scalar potential  $\chi$  associated to primal nodes  $n \in D_c$ .

Using the discrete geometric approach, Maxwell's laws can be written *exactly* as topological balance equations between DoFs arrays as

$$\mathbf{C}^T \mathbf{F} = \mathbf{I}, \tag{1a}$$

$$\Phi = \mathbf{C} \mathbf{A}, \tag{1b}$$

$$\mathbf{G}^T \mathbf{I} = 0, \tag{1c}$$

where (1a) is the Ampère's law at discrete level, (1b) assures that Gauss' law at discrete level  $\mathbf{D}\Phi = 0$  is satisfied identically (since  $\mathbf{D}\mathbf{C} = 0$  holds) and (1c) is the continuity law.

The discrete counterpart of the constitutive laws can be written as

$$\mathbf{F} = \boldsymbol{\nu} \Phi, \quad \text{in } D, \tag{2a}$$

$$\mathbf{I} = \boldsymbol{\sigma} \mathbf{U}, \quad \text{in } D_c. \tag{2b}$$

The square matrix  $\boldsymbol{\nu}$  ( $\dim(\boldsymbol{\nu}) = N_f, N_f$  being the number of faces in  $\mathcal{K}^S$ ) is the reluctance matrix such that (2a) holds exactly at least for an element-wise *uniform* induction field  $\mathbf{B}$  and magnetic field  $\mathbf{H}$  in each tetrahedron and it is the approximate discrete counterpart of the constitutive relation  $\mathbf{H} = \boldsymbol{\nu} \mathbf{B}$  at continuous level,  $\boldsymbol{\nu}$  being the reluctivity assumed element-wise a constant. The square matrix  $\boldsymbol{\sigma}$  ( $\dim(\boldsymbol{\sigma}) = N_e, N_e$  being the number of edges in  $D_c$ ) is the conductance matrix such that (2b) holds exactly at least for an element-wise *uniform* electric field  $\mathbf{E}$  and current density  $\mathbf{J}$  in each tetrahedron and it is the approximate discrete counterpart of the constitutive relation  $\mathbf{J} = \boldsymbol{\sigma} \mathbf{E}$  at continuous level,  $\boldsymbol{\sigma}$  being the conductance assumed element-wise a constant. The construction of the constitutive matrices  $\boldsymbol{\nu}$  and  $\boldsymbol{\sigma}$  will be described in detail in Section 2.4.

Next, we recall the discrete Faraday's law in the frequency domain  $\mathbf{C}\mathbf{U} = -i\omega\mathbf{\Phi}$ , and using (1b), we may write

$$\mathbf{U} = -i\omega(\mathbf{A} + \mathbf{G}\boldsymbol{\chi}), \quad (3)$$

since  $\mathbf{C}\mathbf{G} = 0$  holds identically.

By substituting (2a), (2b), (3) and (1b) in (1a) we obtain the algebraic equations in a one-to-one correspondence with the edges and substituting (2b) and (3) in (1b) we obtain the algebraic equations in a one-to-one correspondence with conductor's nodes. The final algebraic system, having  $\mathbf{A}$  and  $\boldsymbol{\chi}$  as unknowns DoFs arrays, can be written as

$$\begin{aligned} (\mathbf{C}^T \boldsymbol{\nu} \mathbf{C} \mathbf{A})_e &= 0 & \forall e \in D_a, \\ (\mathbf{C}^T \boldsymbol{\nu} \mathbf{C} \mathbf{A})_e &= (\mathbf{I}_s)_e & \forall e \in D_s, \\ (\mathbf{C}^T \boldsymbol{\nu} \mathbf{C} \mathbf{A})_e + i\omega(\boldsymbol{\sigma} \mathbf{A}_c)_e + i\omega(\boldsymbol{\sigma} \mathbf{G} \boldsymbol{\chi})_e &= 0 & \forall e \in D_c, \\ i\omega(\mathbf{G}^T \boldsymbol{\sigma} \mathbf{A}_c)_n + i\omega(\mathbf{G}^T \boldsymbol{\sigma} \mathbf{G} \boldsymbol{\chi})_n &= 0 & \forall n \in D_c, \end{aligned} \quad (4)$$

where array  $\mathbf{A}_c$  is the sub-array of  $\mathbf{A}$ , associated with primal edges in  $D_c$ . With notation  $(x)_k$ , we mean the  $k$ th row of array  $x$ , where  $k = \{e, n\}$  is the label of edge  $e$  or of node  $n$ .

To close the problem, the boundary conditions must be specified; we impose a zero  $\mathbf{A}$  on the primal edges  $e$  on the boundary of  $D$ . System (4) is singular and, to solve it, we rely on conjugate gradient (CG) method without gauge condition [23].

### 3.3 $T$ - $\Omega$ formulation

In  $D$  we consider the mesh  $\mathcal{M}''$  and we refer all the incidence matrices to the simplicial complex  $\tilde{\mathcal{K}}^s$ . We denote with:

- $\mathbf{T}$  the array of the circulations of the electric vector potential  $T$  along  $\tilde{e} \in D_c \cup D_s$ . In  $D_s$  we introduce the array  $\mathbf{T}_s$  of impressed electric vector potential;
- $\mathbf{\Omega}$  the array of magnetic scalar potential  $\Omega$  associated with dual nodes  $\tilde{n} \in D$ .

Again, according to the discrete geometric approach, Maxwell's laws can be written *exactly* as topological balance equations between DoFs arrays as

$$\tilde{\mathbf{G}}^T \mathbf{\Phi} = 0, \quad (5a)$$

$$\mathbf{F} = \tilde{\mathbf{G}} \mathbf{\Omega} + \mathbf{T}, \quad (5b)$$

$$\tilde{\mathbf{C}}^T \mathbf{U} = -i\omega \mathbf{\Phi}, \quad (5c)$$

where (5a) is the Gauss' magnetic law at discrete level and (5c) is the Faraday's law. We search for an array  $\mathbf{T}$  such that  $\tilde{\mathbf{C}} \mathbf{T} = \mathbf{I}$ ; in this way continuity law  $\tilde{\mathbf{D}} \mathbf{I} = 0$  is identically satisfied. In  $D_s$  the circulation of the electric vector potential  $T$  has a prescribed value calculated in such a way that  $\tilde{\mathbf{C}} \mathbf{T}_s = \mathbf{I}_s$ . Finally, (5b) satisfies Ampère's law ( $\tilde{\mathbf{C}} \mathbf{F} = \mathbf{I}$ ) identically since  $\tilde{\mathbf{C}} \tilde{\mathbf{G}} = 0$ .

The discrete counterpart of the constitutive laws can be written as

$$\mathbf{\Phi} = \boldsymbol{\mu} \mathbf{F}, \quad \text{in } D, \quad (6a)$$

$$\mathbf{U} = \boldsymbol{\rho} \mathbf{I}, \quad \text{in } D_c. \quad (6b)$$

The square matrix  $\boldsymbol{\rho}$  ( $\dim(\boldsymbol{\rho}) = N_{f_c}, N_{f_c}$  being the number of faces of  $\mathcal{K}^s$  in  $D_c$ ) is the resistivity matrix such that (6b) holds exactly at least for an element-wise *uniform* current density field  $\mathbf{J}$  and electric field  $\mathbf{E}$  in each tetrahedron and it is the approximate discrete counterpart of the constitutive relation  $\mathbf{E} = \boldsymbol{\rho}\mathbf{J}$  at continuous level,  $\rho$  being the resistivity assumed element-wise a constant. The square matrix  $\boldsymbol{\mu}$  ( $\dim(\boldsymbol{\mu}) = N_e, N_e$  being the number of edges in  $D$ ) is the permeance matrix such that (6a) holds exactly at least for an element-wise *uniform* magnetic field  $\mathbf{H}$  and induction field  $\mathbf{B}$  in each tetrahedron and it is the approximate discrete counterpart of the constitutive relation  $\mathbf{B} = \boldsymbol{\mu}\mathbf{H}$  at continuous level,  $\mu$  being the permeability assumed element-wise a constant. The construction of the constitutive matrices  $\boldsymbol{\rho}$  and  $\boldsymbol{\mu}$  will be described in detail in Section 2.4.

By substituting (6a) and (6b) in (5a) we obtain the algebraic equations in a one-to-one correspondence with the nodes in  $D_c$  and  $D_s$  and substituting (6a), (6b) and Ampère's law  $\tilde{\mathbf{C}}\mathbf{F} = \mathbf{I}$  in (5b) we obtain the algebraic equations in a one-to-one correspondence with the conductor's edges. The final algebraic system, having  $\mathbf{T}$  and  $\boldsymbol{\Omega}$  as unknowns DoFs arrays, becomes

$$\begin{aligned} (\tilde{\mathbf{G}}^T \boldsymbol{\mu} \tilde{\mathbf{G}} \boldsymbol{\Omega})_{\tilde{n}} &= 0 \quad \forall \tilde{n} \in D_a, \\ (\tilde{\mathbf{G}}^T \boldsymbol{\mu} \tilde{\mathbf{G}} \boldsymbol{\Omega})_{\tilde{n}} &= -(\tilde{\mathbf{G}}^T \boldsymbol{\mu} \mathbf{T}_s)_{\tilde{n}} \quad \forall \tilde{n} \in D_s, \\ (\tilde{\mathbf{G}}^T \boldsymbol{\mu} \tilde{\mathbf{G}} \boldsymbol{\Omega})_{\tilde{n}} + (\tilde{\mathbf{G}}^T \boldsymbol{\mu} \mathbf{T})_{\tilde{n}} &= 0 \quad \forall \tilde{n} \in D_c, \\ (\tilde{\mathbf{C}}^T \boldsymbol{\rho} \tilde{\mathbf{C}} \mathbf{T})_{\tilde{e}} + iw(\boldsymbol{\mu}(\mathbf{T} + \tilde{\mathbf{G}} \boldsymbol{\Omega}))_{\tilde{e}} &= 0 \quad \forall \tilde{e} \in D_c. \end{aligned} \quad (7)$$

To compute the array  $\mathbf{T}_s$  from  $\mathbf{I}_s$ , the technique described in [15] can be used. The boundary conditions must be specified;  $\mathbf{T}$  on the dual edges  $\tilde{e}$  on the boundary of  $D_c$  must be zero to avoid a current flow from the conductor domain to air domain. System (7) is singular and, to solve it, we rely on CG method without gauge condition.

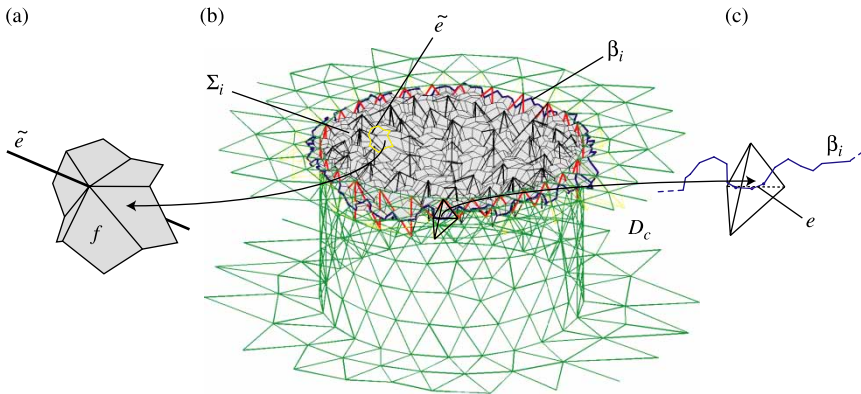


Figure 4. (a) a dual edge  $\tilde{e}$  and the one-to-one corresponding face  $f$ ; (b) a schematic representation of a boundary portion of a conductor domain  $D_c$  with a hole and the relative thick cut. Each primal face  $f$  composing the cut surface  $\Sigma_i$  is the dual of the thick cut edge  $\hat{e}$ ; (c) the boundary of  $\Sigma_i$  is the line  $\beta_i$  composed by primal edges  $e$ .

### 3.3.1 $T$ - $\Omega$ formulation with multiply connected regions

It is well known that in the case of multiply connected regions [14], the m.m.f.s along dual edges  $\tilde{e} \in D_a$  cannot be described completely by the magnetic scalar potential alone. Therefore, according to the classical approach of the *thick cuts*, we extend the definition of the circulations  $\mathbf{T}$  of the electric vector potential along the dual edges  $\tilde{e} \in D_a$  belonging to the so-called thick cuts regions  $D_{tc}$ . Algorithms to compute  $D_{tc}$  can be found in [17] and [18].

In Figure 4(a), a dual edge  $\tilde{e}$  and the one-to-one corresponding face  $f$  are shown. A surface obtained by the union of all primal faces  $f$  in one-to-one correspondence with dual edges  $\tilde{e}$  belonging to each thick cut region of  $D_{tc}$  is called *cut surface*. In Figure 4(b), a possible cut surface  $\Sigma_i$  is depicted in grey and it consists of a collection of a number of primal faces  $f$ . In Figure 4(c), a portion of the boundary  $\beta_i$  of  $\Sigma_i$ , composed by primal edges  $e$ , is shown. A formal and detailed description of the formulation is presented in [19], we recall it briefly.

In the case of non-simply connected conductor regions the domain  $D_{tc}$  exists and, to complete the linear system of equations, additional equations are needed, since additional unknowns DoFs  $(\mathbf{T})_{\tilde{e}}$ , with  $\tilde{e} \in D_{tc}$ , are present. For each cut surface, a *non-local* Faraday law (5c) has to be written involving the cut surface  $\Sigma_i$  and its boundary  $\beta_i$ :

$$\sum_{e \in \beta_i} s_e (\boldsymbol{\rho} \tilde{\mathbf{C}} \mathbf{T})_e = -i\omega \sum_{f \in \Sigma_i} s_f (\boldsymbol{\mu} (\mathbf{T} + \tilde{\mathbf{G}} \boldsymbol{\Omega}))_f,$$

where  $s_e$  is the incidence number ( $\pm 1$ ) between the inner orientations of  $\beta_i$  and the primal edge  $e \in \beta_i$  and  $s_f$  is the incidence number ( $\pm 1$ ) between the inner orientations of the cut surface  $\Sigma_i$  and the inner orientation of the primal face  $f \in \Sigma_i$ .

The other missing equations have to enforce the circulation of the electric vector potential along all homologous paths in  $D_a \cup D_{tc}$  to have the same value, because the circulation have to match the linked current according to the Ampère's law. This is obtained imposing that the circulation of electric vector potential associated with dual edges belonging to  $\Sigma_i$  to be the same, since  $T = 0$  holds outside the thick cut region.

Finally, the boundary conditions to impose are  $(\mathbf{T})_{\tilde{e}} = 0$  on  $\tilde{e} \in \partial(D_c \cup D_{tc})$ .

### 3.4 Construction of the constitutive matrices

Classical ways to construct the constitutive matrices  $\boldsymbol{\nu}$ ,  $\boldsymbol{\rho}$  and  $\boldsymbol{\sigma}$ ,  $\boldsymbol{\mu}$ , are the discrete Hodge technique based on Whitney's maps, described in [9] or the so called Galerkin Hodge [6], that produce the same stiffness matrix as the finite elements with first order edge element basis functions. With the first solution the obtained matrix is non-symmetric, but it is possible to demonstrate that, if the Whitney's functions are evaluated in the bary centre of the tetrahedron the matrix  $\boldsymbol{\sigma}$  becomes symmetric [10].

Here, we will consider another original solution that uses the edge and face vector base functions defined in [11–13]. As proven in the above cited papers, these base functions assure that symmetry, positive-definiteness, and consistency<sup>3</sup> properties are satisfied for all constitutive matrices.

To construct  $\boldsymbol{\mu}$  and  $\boldsymbol{\rho}$ , we will refer to a single tetrahedron  $\tilde{v}$  with a uniform permeability  $\mu$  or resistivity  $\rho$ ; the constitutive matrices for the overall mesh of tetrahedra are obtained by summing up the contributions from the single elements. We will denote with  $\tilde{n}$  the four dual nodes of tetrahedron  $\tilde{v}$  and with  $v$  the four primal volumes in  $\tilde{v}$ ; each  $v$  is a hexahedron in a one-to-one correspondence with a node  $\tilde{n}$ . We denote with  $V$  the volume of  $\tilde{v}$ .

### 3.4.1 Resistance constitutive matrix

The entries of matrix  $\boldsymbol{\rho}$ , of dimension  $4 \times 4$  for tetrahedron  $\tilde{v}$ , are computed as

$$\boldsymbol{\rho}_{ij} = \int_{\tilde{v}} \mathbf{v}_{\tilde{f}_i} \cdot \boldsymbol{\rho} \mathbf{v}_{\tilde{f}_j} \, dv, \quad (8)$$

where  $\mathbf{v}_{\tilde{f}_i}$  is the face vector function associated with the dual face  $\tilde{f}_i$  of tetrahedron  $\tilde{v}$ ; the nodes of the face  $\tilde{f}_i$  are denoted with  $\tilde{n}_a, \tilde{n}_b, \tilde{n}_c$ , respectively. The support of  $\mathbf{v}_{\tilde{f}_i}$  is the union of the three primal volumes having a non-null intersection with face  $\tilde{f}_i$ ; we denote these primal volumes as  $v_a, v_b, v_c$  and the corresponding dual nodes as  $\tilde{n}_a, \tilde{n}_b, \tilde{n}_c$ , respectively. We also denote with  $\tilde{e}_r, \tilde{e}_s, \tilde{e}_t$ , the edge vectors associated with edges  $\tilde{e}_r, \tilde{e}_s, \tilde{e}_t$ , drawn from the nodes  $\tilde{n}_a, \tilde{n}_b, \tilde{n}_c$ , and not belonging to the boundary of  $\tilde{f}_i$ .

Then, the face vector function  $\mathbf{v}_{\tilde{f}_i}$  attached to  $\tilde{f}_i$  is defined as

$$\mathbf{v}_{\tilde{f}_i}(p) = \begin{cases} \tilde{D}_{\tilde{v}i} \tilde{G}_{ra} \frac{\tilde{e}_r}{3V}, & \text{if } p \in v_a, \\ \tilde{D}_{\tilde{v}i} \tilde{G}_{sb} \frac{\tilde{e}_s}{3V}, & \text{if } p \in v_b, \\ \tilde{D}_{\tilde{v}i} \tilde{G}_{tc} \frac{\tilde{e}_t}{3V}, & \text{if } p \in v_c, \end{cases} \quad (9)$$

where  $\tilde{D}_{\tilde{v}i}$  is the incidence number between outer orientations of the pair  $\tilde{v}$  and  $\tilde{f}_i$ ;  $\tilde{G}_{ra}$  is the incidence number between outer orientations of the pair  $\tilde{e}_r, \tilde{n}_a$  and similarly for the others.

### 3.4.2 Permeance constitutive matrix

The entries of matrix  $\boldsymbol{\mu}$ , of dimension  $6 \times 6$  for tetrahedron  $\tilde{v}$ , are computed as

$$\boldsymbol{\mu}_{ij} = \int_{\tilde{v}} \mathbf{v}_{\tilde{e}_i} \cdot \boldsymbol{\mu} \mathbf{v}_{\tilde{e}_j} \, dv, \quad (10)$$

where  $\mathbf{v}_{\tilde{e}_i}$  is the edge vector function associated with the dual edge  $\tilde{e}_i$  of tetrahedron  $\tilde{v}$ ; the nodes of the edge  $\tilde{e}_i$  are denoted with  $\tilde{n}_a, \tilde{n}_b$ , respectively. The support of  $\mathbf{v}_{\tilde{e}_i}$  is the union of the two primal volumes having a non-null intersection with edge  $\tilde{e}_i$ ; we denote these primal volumes as  $v_a, v_b$  and the corresponding dual nodes as  $\tilde{n}_a, \tilde{n}_b$ , respectively. We also denote with  $\tilde{f}_r, \tilde{f}_s$  the face vectors<sup>4</sup> associated with the faces  $\tilde{f}_r, \tilde{f}_s$ . The face  $\tilde{f}_r$  has one vertex only coincident with the node  $\tilde{n}_a$  and the face  $\tilde{f}_s$  has one vertex only coincident with the node  $\tilde{n}_b$ .

Then, the edge vector function  $\mathbf{v}_{\tilde{e}_i}$  attached to  $\tilde{e}_i$  is defined as

$$\mathbf{v}_{\tilde{e}_i}(p) = \begin{cases} \tilde{G}_{ia} \tilde{D}_{\tilde{v}r} \frac{\tilde{f}_r}{3V}, & \text{if } p \in v_a \\ \tilde{G}_{ib} \tilde{D}_{\tilde{v}s} \frac{\tilde{f}_s}{3V}, & \text{if } p \in v_b, \end{cases} \quad (11)$$

where  $\tilde{G}_{ia}$  is the incidence number between  $\tilde{e}_i$  and  $\tilde{n}_a$ ,  $\tilde{D}_{\tilde{v}r}$  is the incidence number between  $\tilde{v}$  and  $\tilde{f}_r$ .

### 3.4.3 Reluctance and conductance matrices

Since both  $\mathbf{v}$  and  $\boldsymbol{\rho}$  are defined using face functions, while  $\boldsymbol{\sigma}$  and  $\boldsymbol{\mu}$  are defined using edge functions, we can calculate  $\mathbf{v}$  and  $\boldsymbol{\sigma}$  from the previous formulas with:

$$\mathbf{v}_{ij} = \int_{\tilde{v}} \mathbf{v}_{\tilde{f}_i} \cdot \nu \mathbf{v}_{\tilde{f}_j} d\nu, \quad (12)$$

and

$$\boldsymbol{\sigma}_{ij} = \int_{\tilde{v}} \mathbf{v}_{\tilde{e}_i} \cdot \boldsymbol{\sigma} \mathbf{v}_{\tilde{e}_j} d\nu, \quad (13)$$

so, for example,  $\mathbf{v}$  and  $\boldsymbol{\rho}$  differ only by the material constant that is element-wise uniform by hypothesis.

## 3.5 Integral representation of sources

### 3.5.1 $A-\chi$

Thanks to the linearity of media, we can express the array  $\mathbf{A}$  as  $\mathbf{A} = \mathbf{A}_r + \mathbf{A}_s$ , where  $\mathbf{A}_s$  is the array of circulations of the contribution to the magnetic vector potential produced by the source currents in  $D_s$  and  $\mathbf{A}_r$  is the array of circulations of the contribution to the magnetic vector potential due to the eddy-currents in  $D_c$ . Therefore, we have that

$$\begin{aligned} (\mathbf{C}^T \boldsymbol{\nu} \mathbf{C} \mathbf{A}_s)_e &= (\mathbf{I}_s)_e & (\mathbf{C}^T \boldsymbol{\nu} \mathbf{C} \mathbf{A}_r)_e &= 0 & \forall e \in D_s, \\ (\mathbf{C}^T \boldsymbol{\nu} \mathbf{C} \mathbf{A}_s)_e &= 0 & (\mathbf{C}^T \boldsymbol{\nu} \mathbf{C} \mathbf{A}_r)_e &= (\mathbf{I})_e & \forall e \in D_c, \end{aligned} \quad (14)$$

holds where  $\mathbf{I}$  is the array of eddy-currents crossing  $\tilde{f}$  in  $D_c$ . Each entry  $(\mathbf{A}_s)_i$  of the array  $\mathbf{A}_s$  can be pre-computed as  $(\mathbf{A}_s)_i = \int e_i \mathbf{A}_s \cdot d\mathbf{l}$ , where  $e_i$  is a primal edge in  $D$  and  $\mathbf{A}_s$  is the magnetic vector potential due to the known source current density in  $D_s$ . In our case, we have stranded circular coils and  $\mathbf{A}_s$  can be computed in closed form in terms of the elliptic integrals of the first and second kind [16].

In this way, we can rewrite system (4) by removing the source currents from its right hand side, obtaining

$$\begin{aligned} (\mathbf{C}^T \boldsymbol{\nu} \mathbf{C} \mathbf{A}_r)_e &= 0 & \forall e \in D - D_c, \\ (\mathbf{C}^T \boldsymbol{\nu} \mathbf{C} \mathbf{A}_r)_e + iw(\boldsymbol{\sigma} \mathbf{A}_{cr})_e + iw(\boldsymbol{\sigma} \mathbf{G} \boldsymbol{\chi})_e &= \mathbf{v} & \forall e \in D_c, \\ iw(\mathbf{G}^T \boldsymbol{\sigma} \mathbf{A}_{cr})_n + iw(\mathbf{G}^T \boldsymbol{\sigma} \mathbf{G} \boldsymbol{\chi})_n &= \mathbf{w} & \forall n \in D_c, \end{aligned} \quad (15)$$

where  $\mathbf{v} = -iw(\boldsymbol{\sigma} \mathbf{A}_{cs})_e$  and  $\mathbf{w} = iw(\mathbf{G}^T \boldsymbol{\nu})_e$ .

### 3.5.2 $T-\Omega$

In order to avoid the specification of the array  $\mathbf{T}_s$  in (7), we adopt an integral representation of the effect of the source currents in  $D_s$ . Thanks to the linearity of media, we can express the DoF array  $\mathbf{F}$  of m.m.f.s along dual edges as  $\mathbf{F} = \mathbf{F}_s + \mathbf{F}_r$ , where  $\mathbf{F}_s$  is the array of m.m.f.s produced by the source currents in  $D_s$  and  $\mathbf{F}_r$  is the array of m.m.f.s due to the eddy-currents in  $D_c$ . Each entry  $F_s$  of the array  $\mathbf{F}_s$  can be computed as  $F_s = \int_{\tilde{e}} \mathbf{H}_s \cdot d\mathbf{l}$ , where  $\mathbf{H}_s$  is the magnetic field expressed by the Biot–Savart law from the source currents in  $D_s$  and  $\tilde{e}$  is a dual edge. Applying Ampere’s law

we have that

$$\begin{aligned}
(\tilde{\mathbf{C}}\mathbf{F}_s)_{\tilde{f}} &= (\mathbf{I}_s)_{\tilde{f}} \quad (\tilde{\mathbf{C}}\mathbf{F}_r)_{\tilde{f}} = 0 \quad \forall \tilde{f} \in D_s, \\
(\tilde{\mathbf{C}}\mathbf{F}_s)_{\tilde{f}} &= 0 \quad (\tilde{\mathbf{C}}\mathbf{F}_r)_{\tilde{f}} = (\mathbf{I}_{\tilde{f}})_{\tilde{f}} \quad \forall \tilde{f} \in D_c, \\
(\tilde{\mathbf{C}}\mathbf{F}_s)_{\tilde{f}} &= 0 \quad (\tilde{\mathbf{C}}\mathbf{F}_r)_{\tilde{f}} = 0 \quad \forall \tilde{f} \in D_a \cup D_{tc}.
\end{aligned} \tag{16}$$

Therefore, the following potentials can be used:  $(\mathbf{F}_r)_{\tilde{e}} = (\tilde{\mathbf{G}}\mathbf{\Omega})_{\tilde{e}}$  with  $\tilde{e} \in (D_a - D_{tc}) \cup D_s$  and  $(\mathbf{F}_r)_{\tilde{e}} = (\mathbf{T}_r + \tilde{\mathbf{G}}\mathbf{\Omega})_{\tilde{e}}$  with  $\tilde{e} \in D_c \cup D_{tc}$ , where  $\mathbf{T}_r$  is the array of the circulation of the electric vector potential due to the eddy-currents in  $D_c$ . Therefore, (7) can be rewritten, respectively, as

$$\begin{aligned}
(\tilde{\mathbf{G}}^T \boldsymbol{\mu} \tilde{\mathbf{G}} \mathbf{\Omega})_{\tilde{n}} &= -(\tilde{\mathbf{G}}^T \boldsymbol{\mu} \mathbf{F}_s)_{\tilde{n}} \quad \forall \tilde{n} \in (D_a - D_{tc}), \\
(\tilde{\mathbf{G}}^T \boldsymbol{\mu} \tilde{\mathbf{G}} \mathbf{\Omega})_{\tilde{n}} + (\tilde{\mathbf{G}}^T \boldsymbol{\mu} \mathbf{T}_c)_{\tilde{n}} &= -(\tilde{\mathbf{G}}^T \boldsymbol{\mu} \mathbf{F}_s)_{\tilde{n}} \quad \forall \tilde{n} \in D_c \cup D_{tc} \cup D_s, \\
(\tilde{\mathbf{C}}^T \boldsymbol{\rho} \tilde{\mathbf{C}} \mathbf{T}_c)_{\tilde{e}} + iw \boldsymbol{\mu} (\mathbf{T}_c + \tilde{\mathbf{G}} \mathbf{\Omega})_{\tilde{e}} &= -iw (\boldsymbol{\mu} \mathbf{F}_s)_{\tilde{e}} \quad \forall \tilde{e} \in D_c.
\end{aligned} \tag{17}$$

In the case of non-simply connected conductor region, the domain  $D_{tc}$  exists and, like we already showed, additional equations have to be written for each dual edge  $\tilde{e} \in D_{tc}$  [19].

### 3.6 Calculation of the induced voltage

For the calculation of the induced voltage with both formulations, we sub-divide the coil in a series of  $M$  sub-coils. Each sub-coil has a cross-section area  $S_i$  such that  $\sum_{i=1}^M S_i = S$ ,  $S$  being the total area of the cross-section of the coil. The voltage induced at the terminals of the  $i$ th sub-coil can be determined by

$$U_i = -iw\Phi_i = -iwN_i \int_{c_i} \mathbf{A} \cdot d\mathbf{l},$$

where  $c_i$  is the circumference coaxial with the coil and passing through the barycentre of the considered sub-coil and  $\mathbf{A}$  is the total magnetic vector potential;  $N_i$  is the number of turns relative to the  $i$ th sub-coil defined as  $N_i = (S_i/S)N$ ,  $N$  being the total number of turns. The vector potential is calculated in the point  $P$  by

$$\mathbf{A}(P) = \mathbf{A}_s(P) + \mathbf{A}_r(P) = \mathbf{A}_s(P) + \frac{\boldsymbol{\mu}_0}{4\pi} \int_{D_c} \frac{J(P')}{|P - P'|} dV,$$

where  $\mathbf{A}_s$  and  $\mathbf{A}_r$  are the magnetic vector potentials produced in  $P$ , respectively, by the source currents in  $D_s$  and the eddy-currents  $\mathbf{J}$  in  $D_c$ .

## 4. Numerical results

When detecting long defects, a reference signal for each coil is not available, therefore it is not possible to use a differential detection system.

To have an estimate of the expected voltage variations in the coils due to the presence of the defect, we computed the voltage variations  $\Delta U = U_d - U_0$  between the voltage on each coil  $U_d$  when the defect is present and the voltage  $U_0$  on the same coil without the defect present.

To this aim we need to solve a pair of eddy-currents problems with the GAME (geometrical approach for Maxwell equations) code [20] with both  $\mathbf{A} - \boldsymbol{\chi}$  and  $\mathbf{T} - \mathbf{\Omega}$  formulations and integral

representation of sources. In NDT (nondestructive testing) applications, the GAME code has been validated in [5,21,22].

The defect has been modelled as a volume discretised with a collection of tetrahedra. The unstructured mesh used consists of 218,685 tetrahedrons, 256,984 edges and 37,629 nodes, yielding 285,285 DoF for the  $\mathbf{A}-\boldsymbol{\chi}$  formulation and 222,410 DoF for the  $\mathbf{T}-\boldsymbol{\Omega}$ . The time to solve each linear system, obtained from the same mesh, on a P4 3 GHz laptop, 2 Gb RAM, is 126 s for the  $\mathbf{T}-\boldsymbol{\Omega}$  formulation, while the  $\mathbf{A}-\boldsymbol{\chi}$  formulation takes 176 s.

We apply also the CARIDDI code [8] implementing the integral formulation to the system under test, splitting the current into a perturbed and an unperturbed solution. Due to the symmetry of the excitation and pickup coils with respect to the conductive region, the memory storage and computational time can be reduced by discretising only one-eighth of the steel cylinder. The mesh used for the perturbed solution is localised near the flaw, allowing for both an increase of accuracy and a reduction of the numbers of unknowns.

It is also interesting to test different positions of the defect in relation to the coil's arrangement. Thanks to the integral representation of the sources, instead of moving the defect it is simpler to move the set of coils keeping always the same mesh. In Figure 2(a), one can see the 2 positions of the defect that have been tested:  $D_1$  is the most sensible position (the defect is just under the coil #4) and  $D_2$  is the less sensible position (the defect is between coil #3 and coil #4).

The compared results are shown in Figure 5.

To detect the defect location an inversion technique based on neural networks can be used, thus this configuration has the potential advantage of indicating also the location of the defect.

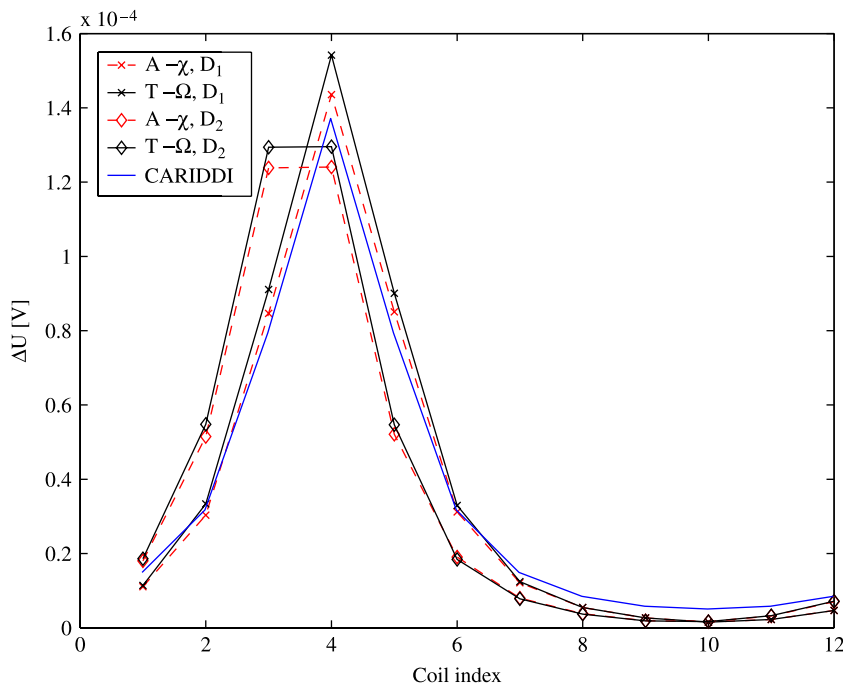


Figure 5. Voltage variation on each of the 12 receiving coils for the two positions of the defect  $D_1$  and  $D_2$ . The numerical results obtained with the GAME and CARIDDI codes are in a good agreement with each other.

## 5. Conclusions

The paper describes two discrete geometric formulations tailored to solve a nondestructive eddy-currents testing problem for the long defect detection during the hot steel-bar production.

The numerical results are in agreement with each other and demonstrate that the two formulations can be considered as useful tools for the numerical modelling and design of eddy-currents diagnostics devices.

In particular it is well known that, like in the framework of Finite Elements, using the average solution obtained by two complementary formulations yields a considerably reduced error in respect to the one obtained using results of each formulation separately.

This motivates an investment in the more complicated, at least when dealing with non-simply connected domains,  $T-\Omega$  formulation.

## Notes

1. These formulations are part of the GAME (geometric approach for Maxwell equations) code developed by R. Specogna and F. Trevisan with the partial support of MIUR (Italian Ministry for University and Research).
2. The minus sign comes from the assumption that inner/outer orientations of a node are opposite.
3. A precise definition of the notion of consistency for constitutive matrices is given in [3].
4. This is a vector normal to the face oriented as the outer orientation of the face and with amplitude equal to the area of the face.

## References

- [1] A. Bossavit, *How weak is the weak solution in finite elements methods?* IEEE Trans. Mag. 34(5) (1998), pp. 2429–2432.
- [2] E. Tonti, *Algebraic topology and computational electromagnetism* (1998), pp. 284–294, 4th International Workshop on Electric and Magnetic Fields, Marseille, France 12–15 May.
- [3] A. Bossavit and L. Kettunen, *Yee-like schemes on staggered cellular grids: A synthesis between FIT and FEM approaches*, IEEE Trans. Mag. 36(4) (2000), pp. 861–867.
- [4] E. Tonti, *Finite formulation of the electromagnetic field*, IEEE Trans. Mag. 38(2) (2002), pp. 333–336.
- [5] F. Trevisan, *3-D eddy current analysis with the cell method for NDE problems*, IEEE Trans. 40(2) (2004), pp. 1314–1317.
- [6] A. Bossavit, *Computational electromagnetism and geometry. (5): The “Galerkin Hodge”*, J. Jpn. Soc. Appl. Electromagn. Mech. 8(2) (2000), pp. 203–209.
- [7] ———, *Geometric interpretation of finite dimensional eddy current formulations*, Int. J. Numer. Meth. Eng. 67(13) (2006), pp. 1888–1908.
- [8] R. Albanese and G. Rubinacci, *Integral formulation for 3D eddy current computation using edge elements*, IEE Proc. 135(5) (1988), pp. 457–462, Part A.
- [9] T. Tarhasaari, L. Kettunen, and A. Bossavit, *Some realizations of a discrete Hodge operator: A reinterpretation of finite element techniques*, IEEE Trans. Mag. 35 (1999), pp. 1494–1497.
- [10] R. Specogna and F. Trevisan, *Discrete constitutive equations in A- $\chi$  geometric eddy-currents formulation*, IEEE Trans. Mag. 41(4) (2005), pp. 1259–1263.
- [11] L. Codecasa, V. Minerva, and M. Politi, *Use of barycentric dual grids for the solution of frequency domain problems by FIT*, IEEE Trans. Mag. 40(2) (2004), pp. 1414–1419.
- [12] L. Codecasa and F. Trevisan, *Piecewise uniform bases and energetic approach for discrete constitutive matrices in electromagnetic problems*, Int. J. Numer. Meth. Eng. 65(4) (2006).
- [13] L. Codecasa, R. Specogna, and F. Trevisan, *Symmetric positive-definite constitutive matrices for discrete eddy-current problems*, IEEE Trans. Mag. 42(2) (2007), pp. 510–515.
- [14] L. Kettunen, K. Forsman, and A. Bossavit, *Formulation of the eddy current problem in multiply connected regions in terms of h*, Int. J. Numer. Meth. Eng. 41(5) (1998), pp. 935–954.
- [15] Y. Le Menach, S. Clenet, and F. Piriou, *Determination and utilization of the source field in 3D magnetostatic problems*, IEEE Trans. Mag. 34(5) (1998), pp. 2509–2512.
- [16] E. Durand, *Magnetostatique*, Masson & C, Paris, 1968.

- [17] Paul W. Gross and P. Robert Kotiuga, *Electromagnetic Theory and Computation: A Topological Approach*, Vol. 48, Cambridge University Press, Cambridge, 2004, ISBN 0 521 801605.
- [18] Saku Suuriniemi, *Homological computations in electromagnetic modeling*, Ph.D. thesis, Tampere University of Technology, 2004, ISBN 952-15-1237-7.
- [19] R. Specogna, Saku Suuriniemi, and F. Trevisan, *Geometric T- $\Omega$  approach to solve eddy-currents coupled to electric circuits*, Int. J. Numer. Meth. Eng., in press, DOI: 10.1002/nme.2155.
- [20] R. Specogna and F. Trevisan, *The geometric approach to solve Maxwell's equations (G.A.M.E.) code*, <http://www.quickgame.org>, copyright 2003–2007.
- [21] E. Cardelli, A. Faba, R. Specogna, A. Tamburrino, F. Trevisan, and S. Ventre, *Analysis methodologies and experimental benchmarks for eddy current testing*, IEEE Trans. Mag. 41(5) (2005), pp. 1380–1383.
- [22] E. Cardelli, A. Faba, R. Specogna, and F. Trevisan, *Image reconstruction of defects in metallic plates using a multi-frequency detector system and a discrete geometric approach*, IEEE Trans. Mag. 42(4) (2007), pp. 1857–1860.
- [23] H. Igarashi and T. Honma, *On convergence of ICCG applied to finite-element equation for quasi-static fields*, IEEE Trans. Mag. 38(2) (2002), pp. 565–568.